

# Nanoscale Chitosan-Based Hemostasis Membrane

Santosh S. Biranje, Pallavi V. Madiwale, Ravindra V. Adivarekar\*

Department of Fibres and Textile Processing Technology, Institute of Chemical Technology, Nathalal Parekh Marg, Matunga, Mumbai, 400 019, India

\*Correspondence should be addressed to R. V. Adivarekar; rv.adivarekar@ictmumbai.edu.in

Received date: September 15, 2020, Accepted date: November 26, 2020

**Copyright:** © 2020 Biranje SS, et al. This is an open-access article distributed under the terms of the Creative Commons Attribution License, which permits unrestricted use, distribution, and reproduction in any medium, provided the original author and source are credited.

## Introduction

Excessive bleeding or hemorrhage in traumatic injuries is the leading preventable cause of death in the combat and civilian trauma centers. Nearly 50% of military deaths, 90% of military battlefield casualties, and 33-56% mortalities in civilian's surgical bleeding are associated with severe bleeding and can be prevented [1]. Hence, significant and rapid hemostasis or bleeding control require innovative strategies with easy to use, stable, and inexpensive processing. Furthermore, the developed hemostatic material should ensure biocompatibility and biodegradability with non-immunogenic properties. To date, a wide variety of hemostatic powders, dressings, and bandages have been investigated as useful materials in reducing hemorrhage. Unfortunately, studies have shown several limitations, especially in managing penetrating injuries, where it is hard to stop bleeding through hemostatic bandages and dressings alone [2]. Also, the most widely used hemostatic powders are still challenging to apply in the wounded area during excessive bleeding [3].

Chitosan is the second most abundant biopolymer after cellulose; it has gained popularity in wound healing applications because of its inherent biocompatibility, biodegradability, antimicrobial, and antifungal properties. The protonated  $\text{NH}_2$  groups of chitosan aggregate blood cells when in contact with blood and form a stable blood clot at the bleeding site to stop bleeding [4,5]. The structural stability of chitosan facilitates the fabrication of varieties of useful structures such as gel, film, powder, membrane, scaffold, patches, sponges, etc. The form and designability mostly determine the efficacy of biopolymer-based hemostatic materials. The porous structure and high surface area of the material promote more interaction with platelets and coagulation factors essential for blood coagulation. Thus, maximizing the chitosan-based hemostatic materials' surface area and porosity will be a

critical initiative for accelerating the hemostasis activity [6].

Recently, chitosan's electrospinning has gained much attention in wound healing applications as it endows with nanofibrous structures in a moderately easy, repeatable, and simple approach [7]. The high surface area and porosity are essential properties of the nanofibrous chitosan that find it extremely efficient for hemostasis application. PVA is a water-soluble polymer and has been shown to produce ultrafine fibres using electrospinning. It has a linear structure and can form hydrogen bonds with polymers similar to many polysaccharides. The spinnability of chitosan can be improved by blending with synthetic biocompatible polyvinyl alcohol (PVA) polymer.

The electrospun membrane can maintain a moist environment at the wound interface to promote cell adhesion and proliferation, essential for wound healing. Also, blood cells and clotting factors can easily be incorporated into the nanofibrous structure to accelerate the coagulation of blood and wound healing [8].

This article discusses the effect of the nanoscale structure of the chitosan-based membrane developed from the electrospun technique and its biological significance on the hemostasis activity. The effect is studied in terms of parameters of biodegradation, bioactivity in terms of hydroxyapatite formation and blood clotting by performing TAT assay.

## Methods

The hemostatic material with a high swelling ability has a larger pore size and surface area, allowing better proliferation or cell attachment. The chitosan/PVA (CH/PVA) membrane's swelling degree is determined as per the reported method [9]. The study of controlled

biodegradation of material is essential for the determination of the time required for tissue growth and skin repair. The biodegradation is determined by *in vitro* incubation of membrane in phosphate buffer containing protease enzyme. Further, the membrane is evaluated for weight loss percentage as per the reported method [9]. The membrane's bioactive property was examined by *in vitro* soaking of the membrane in simulated body fluid (SBF). The hydroxyapatite formed on the dressing surface, upon immersion in SBF, was analyzed by FTIR and XRD study [10]. The *in vitro* blood clotting ability of the membrane was assessed by Thrombin-Antithrombin Complex (TAT) assay. In brief, 3 mL of fresh blood from volunteers was collected in heparin-coated 5 mL Falcon tubes. The scaffold was incubated with 1 mL of blood for 1 h at 37°C. After the incubation period, the plasma was isolated from the blood by centrifugation at 4000 rpm for 20 min, at 28°C. The TAT level in blood samples was measured based on the manufacturer's instructions [<https://www.abcam.com/human-thrombin-antithrombin-complex-elisa-kit-tat-ab108907.html>]. Nitrogen adsorption and desorption isotherm was used to analyze the surface area and pore diameter of the dressing

(ASAP 2010, Micromeritics, USA). The BET specific surface area was determined by the adsorption-desorption data, in the relative pressure (P/P<sub>0</sub>) range of 0.1-0.99.

## Discussion

The swelling property of a biomaterial is vital in regulating cellular activities. The swelling degree increased from 180% to 250% when the mass ratio of CH/PVA was changed from 50/50 to 20/80 as illustrated in Figure 1a. PVA is an excellent water-soluble polymer; the CH/PVA nanofibrous membrane's water uptake could get higher with the increasing amount of PVA [11]. The nanofibrous structure with a more elevated surface to volume ratio of CH/PVA nanofibres enhances the membrane's swelling degree. Also, in the presence of ions in the SBF solution, the electro-neutrality condition increases and creates an additional osmotic pressure that expands the CH/PVA nanofibrous membrane.

The HA's formation on the surface of the CH/PVA nanofibrous membrane was confirmed by FTIR and XRD analysis. In Figure 1c, the characteristic phosphate picks

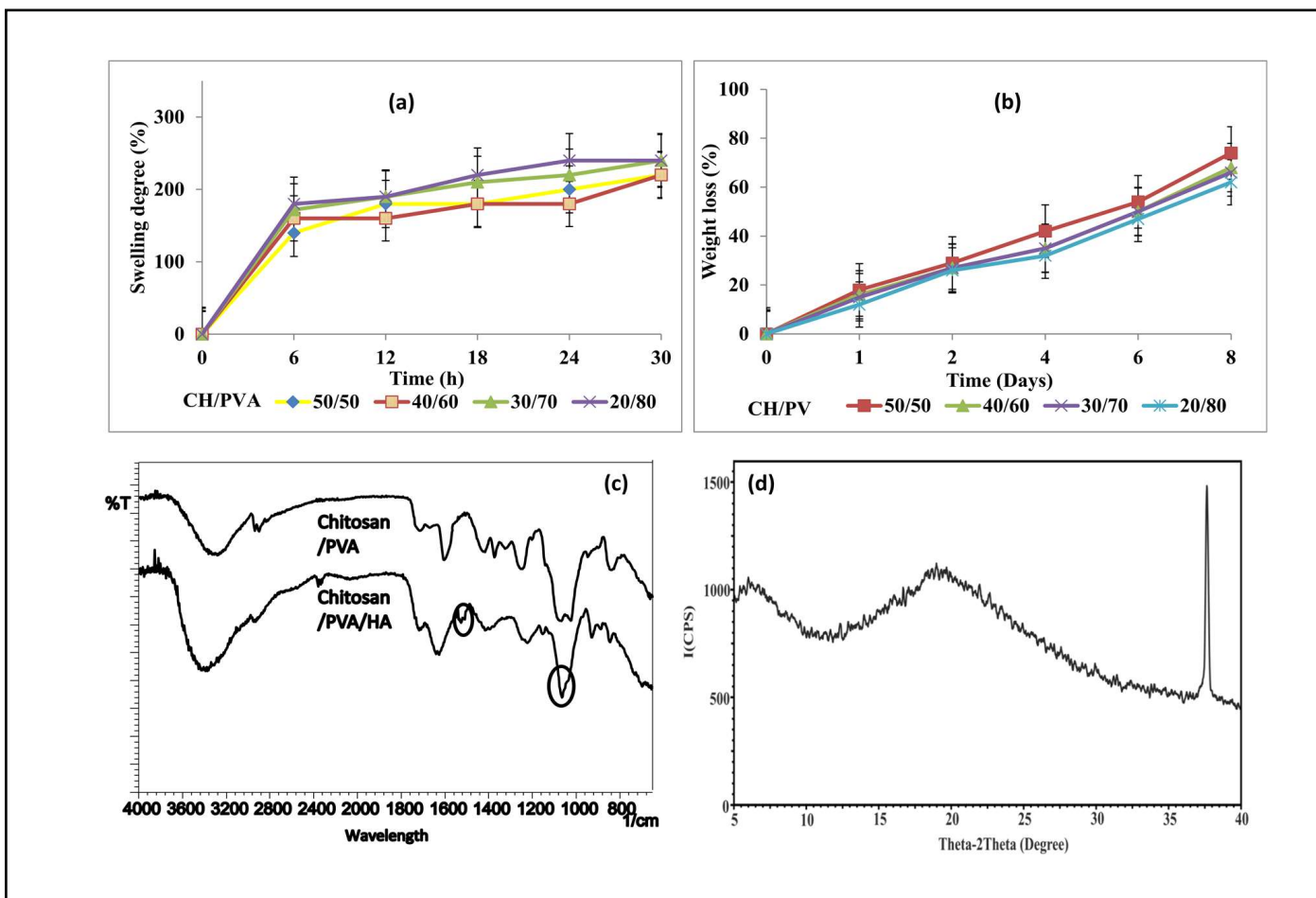


**Figure 1:** Swelling degree (%) (a) and weight loss (%) (b) of electrospun CH/PVA nanofibrous membranes at different mass ratios, FTIR spectra (c) and XRD patterns (d) of SBF incubated CH/PVA nanofibrous membrane.

for HA at a wavenumber of  $1064\text{ cm}^{-1}$  and two peaks at  $1417\text{ cm}^{-1}$  and  $1525\text{ cm}^{-1}$  are probably of the carbonate group, commonly found in synthetic HA and natural bone. In XRD analysis Figure 1d, the broad peak around  $2\theta=20^\circ$  is assigned to chitosan ( $19.6^\circ$ ), and the sharp diffraction characteristic peak at  $36.6^\circ$  corresponds to the peak of HA. Further, the peak intensity of HA increases with increasing the exposure time in SBF. The formation of HA on the surface of the membrane suggests a strong interaction would occur between living tissues and the membrane. After incubation in the SBF solution, numerous tiny hydroxyapatite (HA) particles appeared on the CH/PVA nanofibrous membrane's surface. The chitosan's cationic nature acts as a nucleation site for calcium and phosphate ions present in SBF and further induces HA formation [12,13].

Electrospun CH/PVA nanofibrous membranes have a higher surface area and better water absorption capacity. Therefore all the electrospun membranes exhibited a higher degradation rate. The weight loss analysis has indicated the biodegradation of CH/PVA nanofibrous membrane by protease enzyme, and results are shown in Figure 1b. After 8 days of incubation, CH/PVA nanofibrous membrane with blend ratio 20/80, 30/70, 40/60, 50/50 showed weight losses  $62\pm 2\%$ ,  $66\pm 1\%$ ,  $68\pm 2\%$ , and  $74\pm 2\%$ ,

respectively. The weight loss is lower in CH/PVA (20/80) blend as compared with CH/PVA (50/50), which may be due to a higher proportion of PVA having excellent stability in the water, which does not degrade unless higher temperature conditions ( $\geq 60^\circ\text{C}$ ).

Figure 2b shows the  $\text{N}_2$  adsorption/desorption isotherm and pore size distribution of the CH/PVA nanofibrous membrane. According to the International Union of Pure and Applied Chemistry (IUPAC), it fits into typical type V, which indicates a mesoporous structure. Nanofibrous membranes for wound dressing usually have pore sizes ranging from  $500\text{ nm}$  to  $1\text{ }\mu\text{m}$  and a surface area of  $5\text{--}100\text{ m}^2/\text{gm}$ , which is extremely efficient for fluid absorption and dermal delivery [14]. The adsorption and pore properties of the CH/PVA nanofibrous membrane are calculated from the adsorption-desorption isotherms. BET specific surface area is  $73.7124\text{ m}^2/\text{gm}$ , and the total pore volume of single point adsorption is  $0.132\text{ cc/gm}$ . Since the CH/PVA nanofibrous membrane's surface area is in the required range, they have potential applications for cell attachment and proliferation in wound dressing. The fibres of varying fineness were electrospun from the mixture of CH/PVA with the blend ratio of 10/90 to 50/50. The fibres with diameter  $100\text{--}300 \pm 20\text{ nm}$  were observed and interspersed with enlarged spindle-like widths, as

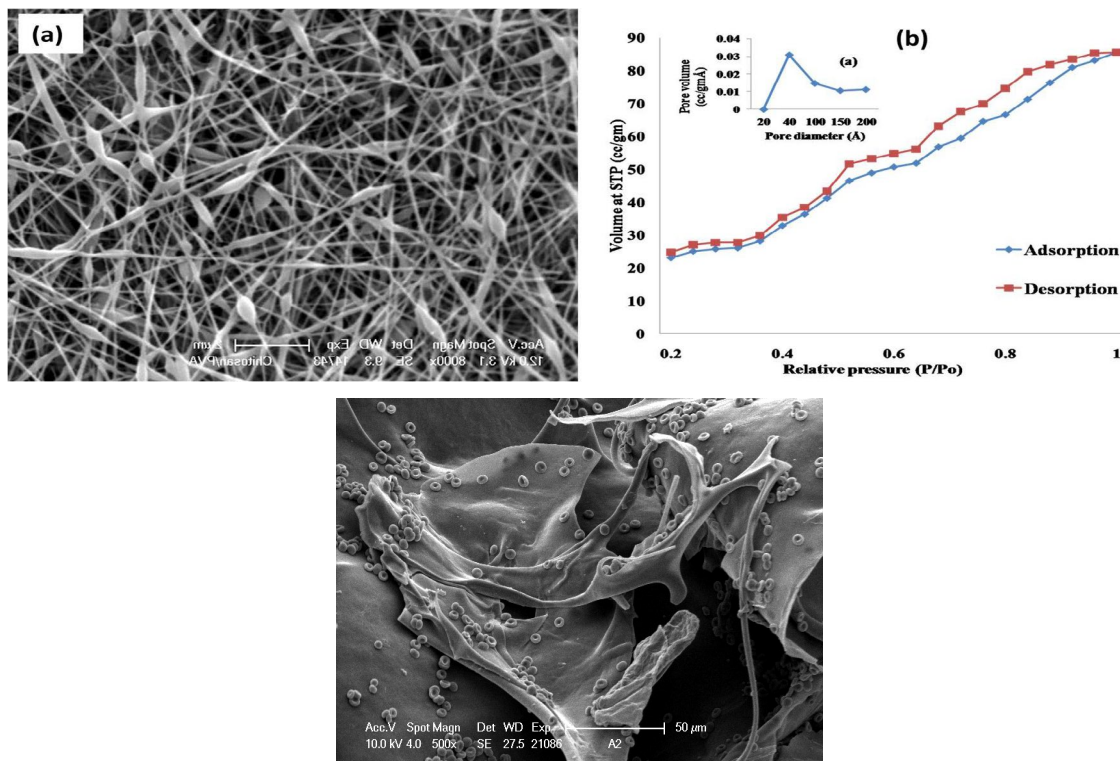


**Figure 2:** Nanofibrous structure (a), Nitrogen adsorption-desorption isotherm (b), SEM image of RBCs adhesion to the CH/PVA nanofibrous membrane (c).



shown in Figure 2a. At the applied potential of 25 kV, with a decrease in chitosan content in CH/PVA blend, the fibre diameter was decreased from 300 nm to 100 nm.

The amino residues of chitosan attract negatively charged red blood cells (RBCs), adsorb fibrinogen, and plasma proteins essential for blood coagulation. It provides active sites to platelets, facilitating primary hemostasis by binding via GPIIb/IIIa to the fibrinogen [15]. The adhesion of the RBCs to the CH/PVA membrane was studied by its *in vitro* incubation with RBCs and analyzed by SEM as shown in Figure 2c. The TAT level in blood contacted with CH/PVA nanofibrous membrane (200-205 ng/mL) was higher than standard (120 ng/mL). The CH/PVA (40/60) blend with higher chitosan content, and the uniform nanofibrous membrane is considered the most optimum combination for reliable hemostasis activity. It can be best suited for application in wound healing dressing. Overall, hemostasis assay results suggest that the CH/PVA nanofibrous membrane can work most optimally for shortening of the blood clotting time and can form a stable blood clot that stops bleeding and faster thrombin generation. The nanofibrous structure and high surface area have the advantage of healthy interactions with platelets and coagulation factors essential for strengthening the blood clots [6].

## Conclusion

The chitosan/PVA nanofibrous membrane are developed with high porosity, enhanced swelling properties, controlled biodegradation, and biocompatibility thus enhancing the wound healing properties. These properties of the membrane also aid in absorbing wound exudates, improving permeability and enhance thrombin generation. The TAT assay demonstrates that the membrane can accelerate hemostasis activity through enhanced thrombin formation, which makes it suitable for blood clotting applications. The high surface area and nanofibrous structure of the CH/PVA membrane offer synergistic coagulation by adsorbing and combining with blood cells. Thus the chitosan/PVA nanofibrous hemostasis membrane has immense potential for wound healing applications.

## Future Perspectives

Overall, chitosan's electrospinning to produce nanofibrous membranes is a good prospect for future research and development of nano/micro porous hemostatic materials for excessive bleeding. Electrospinning enables fabricating several horizontal and vertical structures and weaving the 3D network with the desired configuration to provide excellent support suitable for the bleeding point. However, low production rate and limited clinical application are the main issues in the electrospinning techniques that should be put on our research agenda with the strategical

protocol for an exceptional breakthrough in wound healing hemostasis. The 3D structures incorporated with the novel optical biosensor and stimuli-responsive materials that will sense the status of the wound and release active agents should be taken up in the hemostatic material research for the healing of the wound. A novel next-generation 3D structure hemostat will have benefits of reduction of hospitalization, minimum blood loss and a better understanding of the wound healing process. Along with the development of next-generation, hemostat economic concerns should also be considered for their actual clinical use.

## References

1. Khan MA, Mujahid M. A review on recent advances in chitosan based composite for hemostatic dressings. *International Journal of Biological Macromolecules.* 2019 Mar 1;124:138-47.
2. Hickman DA, Pawlowski CL, Sekhon UD, Marks J, Gupta AS. Biomaterials and advanced technologies for hemostatic management of bleeding. *Advanced Materials.* 2018 Jan;30(4):1700859.
3. Yang X, Liu W, Li N, Wang M, Liang B, Ullah I, et al. Design and development of polysaccharide hemostatic materials and their hemostatic mechanism. *Biomaterials Science.* 2017;5(12):2357-68.
4. Badhe RV, Bijukumar D, Chejara DR, Mabrouk M, Choonara YE, Kumar P, et al. A composite chitosan-gelatin bi-layered, biomimetic macroporous scaffold for blood vessel tissue engineering. *Carbohydrate Polymers.* 2017 Feb 10;157:1215-25.
5. Sundaram MN, Amirthalingam S, Mony U, Varma PK, Jayakumar R. Injectable chitosan-nano bioglass composite hemostatic hydrogel for effective bleeding control. *International Journal Of Biological Macromolecules.* 2019 May 15;129:936-43.
6. Leonhardt EE, Kang N, Hamad MA, Wooley KL, Elsabahy M. Absorbable hemostatic hydrogels comprising composites of sacrificial templates and honeycomb-like nanofibrous mats of chitosan. *Nature Communications.* 2019 May 24;10(1):2307.
7. Ardila N, Medina N, Arkoun M, Heuzey MC, Ajji A, Panchal CJ. Chitosan-bacterial nanocellulose nanofibrous structures for potential wound dressing applications. *Cellulose.* 2016 Oct 1;23(5):3089-104.
8. Ardila N, Medina N, Arkoun M, Heuzey MC, Ajji A, Panchal CJ. Chitosan-bacterial nanocellulose nanofibrous structures for potential wound dressing applications. *Cellulose.* 2016 Oct 1;23(5):3089-104.

9. Biranje SS, Madiwale PV, Patankar KC, Chhabra R, Dandekar-Jain P, Adivarekar RV. Hemostasis and anti-necrotic activity of wound-healing dressing containing chitosan nanoparticles. *International Journal Of Biological Macromolecules*. 2019 Jan 1;121:936-46.

10. Gupta KK, Kundan A, Mishra PK, Srivastava P, Mohanty S, Singh NK, et al. Polycaprolactone composites with TiO<sub>2</sub> for potential nanobiomaterials: tunable properties using different phases. *Physical Chemistry Chemical Physics*. 2012;14(37):12844-53.

11. Bhattarai N, Edmondson D, Veiseh O, Matsen FA, Zhang M. Electrospun chitosan-based nanofibers and their cellular compatibility. *Biomaterials*. 2005 Nov 1;26(31):6176-84.

12. Huang D, Zuo Y, Zou Q, Wang Y, Gao S, Wang X, et al. Reinforced nanohydroxyapatite/polyamide66 scaffolds by chitosan coating for bone tissue engineering. *Journal of Biomedical Materials Research Part B: Applied Biomaterials*. 2012 Jan;100(1):51-7.

13. Kong L, Gao Y, Lu G, Gong Y, Zhao N, Zhang X. A study on the bioactivity of chitosan/nano-hydroxyapatite composite scaffolds for bone tissue engineering. *European Polymer Journal*. 2006 Dec 1;42(12):3171-9.

14. Schiffman JD, Schauer CL. Cross-linking chitosan nanofibers. *Biomacromolecules*. 2007 Feb 12;8(2):594-601.

15. Benesch J, Tengvall P. Blood protein adsorption onto chitosan. *Biomaterials*. 2002 Jun 1;23(12):2561-8.